Article:

Hammond, J., Rosenberg, M. and Brown, S. (2025) Understanding costs in hydrogen infrastructure networks: a multi-stage approach for spatially-aware pipeline design. International Journal of Hydrogen Energy, 102. pp. 430-443. ISSN: 0360-3199

https://doi.org/10.1016/j.ijhydene.2024.12.273

International Journal of Hydrogen Energy 102 (2025) 430–443

Contents lists available at ScienceDirect

International Journal of Hydrogen Energy

journal homepage: www.elsevier.com/locate/he

Understanding costs in hydrogen infrastructure networks: A multi-stage approach for spatially-aware pipeline design

Joseph Hammond [a], Manou Rosenberg [b], Solomon Brown [a,*]

[a] Department of Chemical, Materials & Biological Engineering, The University of Sheffield, Mappin Street, Sheffield, S1 3JD, UK
[b] Curtin Centre for Optimisation and Decision Science, Curtin University, Perth, Australia

A R T I C L E I N F O

Handling Editor: Suleyman I. Allakhverdiev

Keywords:
Hydrogen infrastructure
Pipeline routing with obstacles
Pipeline design optimisation
Genetic algorithm
GIS
Industrial clusters

A B S T R A C T

The emergence and design of hydrogen transport infrastructures are crucial steps towards the development of a hydrogen economy. However, pipeline routing remains underdeveloped in hydrogen infrastructure design models, despite its significant impact on the resultant cost and network configuration. Many previous studies assume uniform cost surfaces on which pipelines are designed. Studies that consider a variable cost surface focus on designing candidate networks rather than bespoke routes for a given infrastructure. This study proposes a novel multi-stage approach based on a graph-based Steiner tree with Obstacles Genetic Algorithm (StObGA) to route pipelines on a complex cost surface for multi-source multi-sink hydrogen networks. The application of StObGA results in cost savings of 20–40% compared to alternative graph-based methods that assume uniform cost surfaces. Furthermore, this publication presents an in-depth methodological comparative analysis of different pipeline routing and sizing methods used in the literature and discusses their impact. Finally, we demonstrate how this model can generate design variations and provide practical insights to inform industry and policymakers.

Abbreviation	Description
StObGA	Steiner tree with obstacles genetic algorithm
IEA	International energy agency
FID	Final investment decision
MST	Minimal spanning tree
CCUS	Carbon capture, utilisation and storage
GIS	Geographic information system
MINLP	Mixed-integer non-linear programming
PSO	Pipeline sizing optimisation
GA	Genetic algorithm
MOP	Maximum operating pressure
REPD	Renewable energy planning database
DPA	Densely populated area
AGI	Above ground installation
LCOHT	Levelised cost of hydrogen transportation
TRL	Technological readiness level
SMR	Steam methane reforming
Symbols	**Description**
ΔP_{ij}	Pressure differential along arc (i, j) (Pa)
κ^{DF}	Design factor
κ^{E}	Longitudinal joint factor
μ	Dynamic viscosity (Pa s)
ρ	Fluid density (kg/m^3)
τ^{p}	Minimum yield stress (Pa)
τ^{w}	Pipeline shear (N/m^2)
Re_{ij}	Reynolds number along arc (i, j)
ξ	Pipe roughness (mm)
a_{ij}	Binary variable indicating existence of arc (i, j)
B_{ijd}	Binary diameter activation variable
C	Total cost of pipeline infrastructure ($ millions)
C_i	Consumption at node i (kg/yr)
C^{C}_{ij}	Capital cost of pipeline along arc (i, j) ($ millions)
D^{si}_{d}	Commercially available inner diameters (m)
D^{so}_{d}	Commercially available outer diameters (m)
D^{pi}_{d}	Inner diameter of pipeline along arc (i, j) (m)
D^{po}_{d}	Outer diameter of pipeline along arc (i, j) (m)
f_{ij}	Friction factor along arc (i, j)
L^{w}_{n}	Weighted length of network n (m)
$L^{obs}_{ij,o}$	Length of arc (i, j) within obstacle o (m)
L_{ij}	Length of pipeline along arc (i, j) (m)
L^{w}_{ij}	Weighted length along arc (i, j) (m)
L^{free}_{ij}	Length of arc (i, j) outside of obstacles (m)
N^{p}_{ij}	Number of parallel pipelines along arc (i, j)

(*continued on next page*)

* Corresponding author.
E-mail address: s.f.brown@sheffield.ac.uk (S. Brown).

https://doi.org/10.1016/j.ijhydene.2024.12.273
Received 27 August 2024; Received in revised form 9 December 2024; Accepted 16 December 2024
Available online 11 January 2025
0360-3199/

(*continued*)

P^{MOP}	Maximum operating pressure (Pa)
P_i	Production at node i (kg/yr)
P_i^{out}	Outflow pressure at node i (Pa)
P_j^{in}	Inflow pressure node j (Pa)
Q_{ij}	Flowrate from node i to j (kg/yr)
Q_{ij}	Total flowrate along arc (i, j) (kg/hr)
Q_{ij}^p	Flowrate through each individual pipe along arc (i, j) (kg/hr)
Q_{ki}	Flowrate from node k to i (kg/yr)
t_{ij}^w	Wall thickness along arc (i, j) (m)
t_{ij}^{wc}	Minimum wall thickness along arc (i, j) (m)
v_{ij}^e	Erosional velocity threshold along arc (i, j) (m/s)
v_{ij}^f	Fluid's velocity along arc (i, j) (m/s)
w_o	Penalty weighting of obstacle o

1. Introduction

Hydrogen offers large industries a versatile alternative energy vector with a high energy density and significant potential for decarbonisation. Produced via renewable sources, it can be used as a combustion fuel that emits only water or directly in chemical processes, offering flexibility in application. However, hydrogen production and adoption remain at a very nascent stage [1], inhibited by unfavourable cost estimates [2] and a circular dependency in its infrastructure dynamics, where producers, consumers, and planners each wait for the others to act first, creating a standstill [3].

The International Energy Agency (IEA) tracks the global progress of infrastructure projects that aim to use hydrogen as an energy carrier or industrial feedstock with the potential of mitigating emissions [4]. In 2023, the IEA found that many projects remain in the concept and feasibility study stages and fail to achieve Final Investment Decisions (FIDs) (see Fig. 1).

Of the global projects, only four have made FIDs. These late-stage projects have planned relatively small pipeline infrastructures below 100 km in total network length, while the only operational project stands at just 12 km. Over half of the projects propose lengths over 100 km with the largest few exceeding 2000 km [5–7], yet none of these have begun to materialise. Given the nascent state of hydrogen infrastructures and the uncertainties in where hydrogen producers and consumers will be located, optimal design models prove particularly useful. They provide a framework for analysing how design requirements shift across different production and uptake scenarios, thereby assisting in strategic planning and implementation [8].

Optimal design models determine the topology and size of the hydrogen infrastructure's pipelines for a given scenario. Many studies use a multi-stage methodology [9–11], segregating the infrastructure's routing and design due to the non-linear relationships between routing constraints, hydraulic gas dynamics, and the length and flow relationships within networks. The first of these elements, determining the infrastructure's topology, requires a spatially-explicit model to ascertain the route and calculate the subsequent pipeline lengths. Simple graph-based methods such as Minimal Spanning Tree (MST) [12,13] and Steiner tree algorithms [8,14] are commonly used to minimise the network length as a proxy for cost. However, minimum-length topologies rarely align with the optimal minimum-cost networks [8,9]. To the authors' knowledge, only André et al. [9] attempt to address this specifically within hydrogen infrastructure design. In their study, they iteratively refine a MST solution by applying various heuristics, costing many topologies then choosing the lowest cost network. The costing includes hydrogen pipeline specific attributes like fluid properties and diameters. More generally, Heijnen et al. [8] proposes an adapted Gilbert-Melzak algorithm to find minimum cost Steiner trees showing similar percentage improvements to the design as André et al. [9] but generalise the problem by using a flow-cost heuristic with no specific considerations of the fluid nor pipeline attributes. Nevertheless, both of these approaches and other studies in the literature [15] assume a uniform cost surface, ignoring geographical variations, that can result in pipelines traversing undesirable or even untraversable areas.

Route design is variable to many geographical obstacles such as slopes, transportation crossings, water bodies, forests, and populated areas. These areas can either be traversed, typically at a higher cost, or evaded [16]. A route should consider areas where traversing is more expensive. Only one study by Heijnen et al. [17] considers a varying cost surface, albeit simply, by applying a multi-step graph-based methodology to find a route around one untraversable obstacle in the routing design. Further complexities such as varying traversable cost surfaces and many obstacles remain to be studied.

Where simple graphs are not used to define the distribution network, studies often utilise pre-defined networks [10,11,18–20], which is apt for some pipeline systems such as residential infrastructure and heat networks that follow roads [21]. Baufumé et al. [10] and Johnson and Ogden [18] use pre-existing infrastructures as templates for their hydrogen network routes. Reuβ et al. [11] explore the impact of using different route topologies generated from a pre-defined candidate network. Parolin et al. [19] utilise a combination of existing roads and the gas grid to design their route. Nevertheless, pre-defined routes are limited in their scope and fall short as a pragmatic tool where existing routes are not appropriate.

Few studies provide a methodology to model pipeline network routing where appropriate infrastructure does not exist or the route is not known. Only one study (Middleton et al. [22]) found by the authors address the creation of candidate pipeline networks with geographical considerations for Carbon Capture Utilisation and Storage (CCUS) infrastructure design. Middleton et al. applies a 5-step process to generate candidate networks on top of grid-based cost surfaces that are quantified based on the topography, land use, ownership, and population density. Then, this candidate network is input as a topological constraint that bounds a network design optimisation model [23].

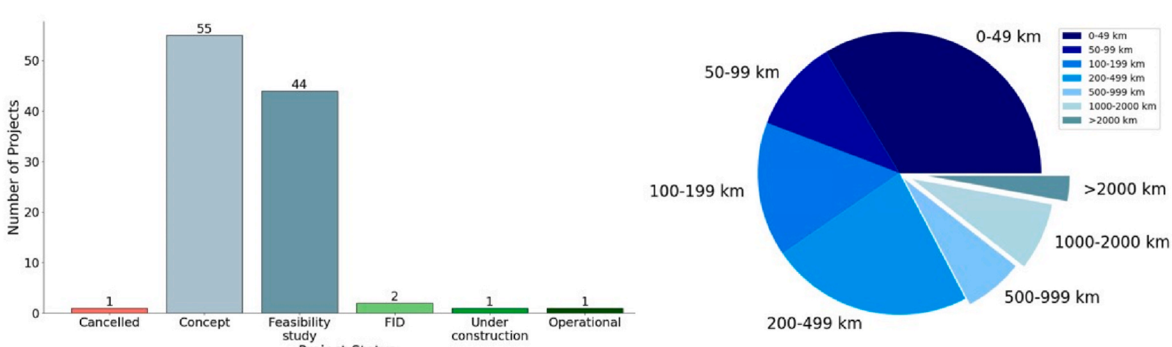

Fig. 1. Left: Bar chart depicting the project status of hydrogen infrastructure projects in Europe. Right: A pie chart presenting the distribution of pipeline network lengths for planned and existing hydrogen infrastructure projects. Data sourced from IEA (2023) [4].

Nevertheless, the generation of a candidate network does not provide an optimal topology for a specific scenario but rather a network structure that scenarios can be mapped upon and then optimised.

The design of an optimised route in grid-based approaches is constrained by the grid's coarseness; for instance, in Middleton et al.'s works [22,24], grids are approximately 1 km × 1 km, which restricts the spatial resolution and limits algorithms' ability to navigate narrow solution spaces where the optimal route may misalign with the grid's discretisation. Moreover, pathfinding methods face difficulties in handling significant discontinuities in the cost surface.

After the routing stage, a subsequent design stage determines the properties of node interconnections. Some studies choose to investigate the different options for transporting hydrogen between locations. Yang and Ogden [25] perform a techno-economic analysis comparing three hydrogen transportation options: liquid trucks, compressed gas trucks, and pipelines; finding that pipelines are generally the most economical transportation option, except for cases of exceptionally low flows or long distances (>500 km). Parolin et al. [19] study competing modalities within an infrastructure design context, demonstrating that the optimal configuration for hydrogen refuelling stations is a mix of truck deliveries and pipelines, saving between 4 and 11% compared to relying exclusively on a single modality in their case study. However, the authors note the high computational costs of including several transport options in the optimisation model. Furthermore, multi-modality models are particularly suited to large networks with smaller flows, such as hydrogen refuelling stations, rather than smaller networks with larger flows, like industrial hydrogen infrastructure, where pipelines are typically more economical and logistically advantageous [25,26].

Other studies focus primarily on pipelines [9,10,27–29], ranging in their complexity. Welder et al. [27] use a fixed gas velocity and linearise pipeline costs for varying hydrogen flows. Baufumé et al. [10] determine the diameter using a simplified flow equation with a fixed velocity and no additional constraints. Other studies [9,28] include the pressure differential within the pipelines and a dynamic velocity, therefore contending with the non-linear relationships between the pressure, velocity and flowrate. A comparative analysis by Reuβ et al. [11] of the two design options argue that fixing the velocity is an acceptable approximation, but discrepancies increase with larger diameters.

Some studies [18,28,30] consider discrete pipeline sizes as an additional constraint, making an allowance for only commercially available sizes. Whereas André et al. [9] size the pipelines with continuous sizes under the pretence that commercial availability may change. Estimating the cost difference between models with discrete and continuous sizing is relatively straight forward, however none of the literature reviewed quantifies this difference.

Many constraint configurations exist for hydrogen network pipeline design. The constraints chosen by a study depend on its scope and computational limitations. Parolin et al. [19] do not define any pipeline attributes within their optimisation; this allows them to incorporate multiple modalities as well as production and storage considerations. Similarly in the CCUS literature, Becattini et al. [15] put little focus on the pipeline design; simply, the pipeline cost is a function of the flow rate through each existing arc. Instead, they incorporate optimal equipment installation and sizing at production and storage sites. On the other hand, studies such as Ejeh et al. [31] focus entirely on pipeline network design which provides them with the computational availability to include hydraulic, structural, and commercial constraints for a given set of pipelines and their corresponding flowrates.

Reducing the complexity of pipeline network routing and design can allow for more decision variables at production, storage and consumption sites. This approach can be a useful tool for policymakers trying to understand the potential impact of new infrastructures, however, these models are limited due to oversimplifying assumptions, particularly to engineers and infrastructure planners. Specifically, these models often assume a centralised planning strategy where equipment, infrastructure and sites are decided in tandem as part of one cohesive problem [32,33]. In reality, infrastructure development is influenced by diverse stakeholders with different objectives and internal environments [34]. Consequently, the emergence of new infrastructures depends significantly on their decisions. Therefore, this study advocates for models that incorporate high-fidelity design stages specific to pipeline networks, as they offer more practical insights and flexibility for experimenting with infrastructure design.

In this paper, we propose a spatially-explicit, multi-stage optimisation model for hydrogen pipeline infrastructure design given industrial sites with Geographic Information System (GIS) coordinates, and production and consumption values. The model's routing stage utilises the Steiner Tree with Obstacles Genetic Algorithm (StObGA) developed by Rosenberg et al. [14] to design the infrastructure's topology with consideration of an array of complex geographical obstacles [35]. StObGA minimises the network's length while navigating both traversable and untraversable obstacles, allowing us to define a cost surface with variable weights based on an area's traversal cost. The subsequent pipeline design stage utilises a Mixed-Integer Non-Linear Programming (MINLP) model to define the pipeline dimensions under hydraulic, structural, and commercial constraints.

Graph-based routing approaches have primarily improved by consolidating the routing and sizing stages to avoid sub-optimal configurations. However, insufficient research has targeted achieving complex topologies that account for geographical constraints. For large-scale infrastructures, the number and variety of geographical obstacles are likely to be large. Many of the hydrogen projects being tracked by the IEA are regional or larger in their scope, so the consideration of obstacles is particularly relevant, yet no studies reviewed explore their impact on the infrastructure's cost. Where cost surfaces have been considered, they have been used to generate candidate networks rather than optimal pipeline infrastructure designs for a select scenario.

This study addresses the identified gaps and advance existing work through the following contributions:

- Propose a novel approach to design bespoke multi-source multi-sink pipeline network infrastructure with geographical constraints.
- Present how the generation of realistic routes significantly changes the topology, thereby reducing the infrastructure costs.
- Quantify the importance of using discrete sizing for hydrogen pipeline networks in industrial clusters.

The remainder of this paper is organised as follows: Section 2 introduces the multi-stage model. Section 3.1 presents a UK-based regional case study. Then, Section 3 details the results and subsequent discussion. Finally Section 4 concludes the study by discussing the key insights and impact of this investigation.

2. Methods and data

The proposed method designs hydrogen pipeline networks by connecting given sets of supply and demand points, while considering geographically constrained areas where pipeline installation incurs a higher cost. The problem is modelled as a graph, with supply and demand points represented as terminal nodes and geographical constrained areas defined as polygonal shapes on the plane. This section introduces three model stages used to design a regional hydrogen infrastructure.

Fig. 2 depicts the method's workflow. First, a route is defined by StObGA. StObGA designs the route around user-defined geographical constraints which are represented as polygons with a given penalty weighting. The use of StObGA allows the model to design the network without the need for a candidate network as seen in other studies, creating a unique and optimised infrastructure route for a given scenario.

The nodes and arcs generated are input into the material balance model, formulated as an optimisation model with a cost-weighted length

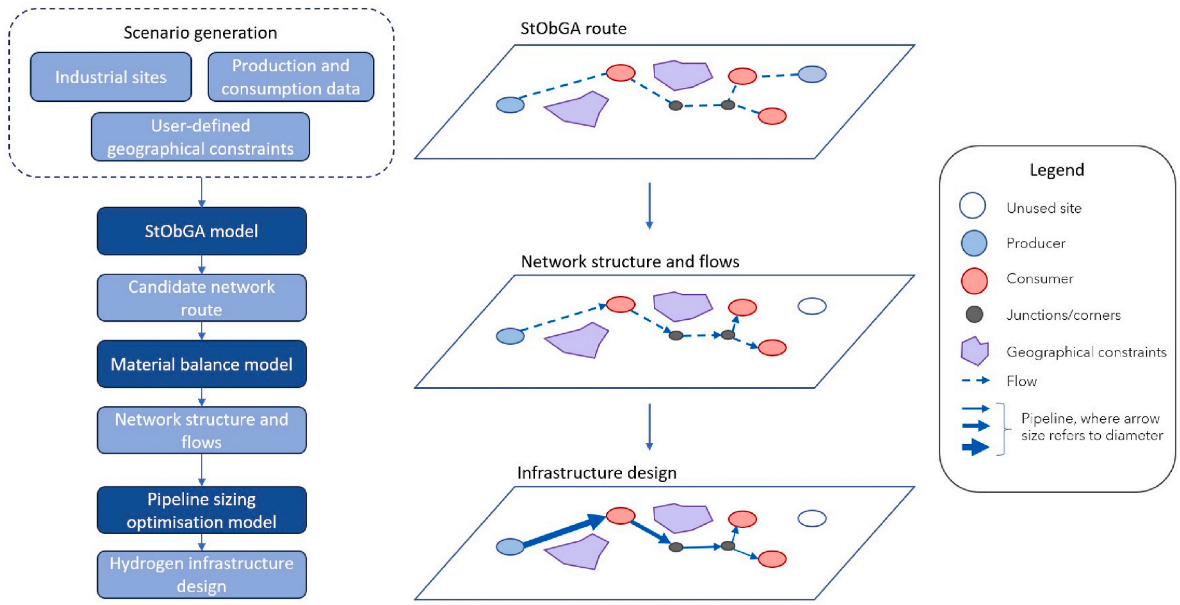

Fig. 2. Methodological workflow with a visual depiction of the consecutive model stages and outputs.

minimisation objective, which is used as a proxy for cost. The material balance model specifies which arcs exist, and their direction and flowrate. Formulating the material balance in a separate model, as opposed to within the Pipeline Sizing Optimisation (PSO) model, provides two advantages:

1. It allows for a more flexible determination of the network structure from StObGA's route, such as the removal of redundant arcs.
2 It enables for more complex pipeline considerations and constraints within the PSO model by reducing the problem's complexity.

The PSO model is a MINLP model that finds the required pipeline diameter while minimising the cost, which is a function of the pipeline's length and outer diameter. The PSO considers hydraulic, structural, velocity, and commercial constraints.

2.1. StObGA

StObGA was first introduced by Rosenberg et al. [14] as a method to solve Euclidean Steiner tree problems with solid (untraversable) and soft (traversable) obstacles. The use of StObGA as the routing method accommodates geographical constraints by representing them as polygonal obstacles with a given penalty weighting. StObGA achieves this by locating Steiner points, as additional junction nodes in the network, and obstacle corner points, that are included in the network routing. These are represented in the genome as shown in 1. The first part of the genome represents the number and x-y coordinates of the Steiner points and is of variable length, and the second part is a fixed-length binary list that determines which corner points of the polygonal obstacles are used in the network.

$$\{(x_1,y_1),(x_2,y_2),(x_3,y_3),\dots,(x_s,y_s)\} + [1\ 0\ 1\ 0\ 0\ 0\ 1\ 1\ 0\ 0] \tag{1}$$

The final network connections are determined using Kruskal's MST algorithm [12], which constructs a minimum spanning tree that includes all terminals, Steiner points, and obstacle nodes. The objective, as described in Equation (2), is to minimise the total weighted length of the arcs; while the genetic algorithm does not directly optimise this function, it is guided to converge towards this goal through length-minimising tournament selection. The weighted length for each arc is calculated as the sum of: (1) the product of the length of any section crossing an obstacle and the corresponding obstacle's penalty weighting, and (2) the length of the section outside any obstacles.

$$\min L_n^w = \sum_{(i,j)\in A}\left(\sum_{o\in O_{ij}} L_{ij,o}^{obs}\cdot w_o + L_{ij}^{\text{free}}\right) \tag{2}$$

Algorithm 1 presents a high-level pseudocode of StObGA. The initial population consists of various genomes that are created using techniques such as Delaunay triangulation to guide Steiner point locations, random generation of Steiner points and obstacle corner activation. New populations are generated in a two-stage process. First, two parent genomes are selected from the population to create a new genome, with part sourced from each parent. Second, each child genome performs one of three mutations: adding or removing Steiner points, activating or deactivating an obstacle corner selection, or shifting the position of Steiner points. After many evolutions, the topology converges to a minimum cost network that defines the infrastructure's route.

Algorithm 1. High-level pseudocode of StObGA

1: Initialisation:
2: Set GA parameters: population size, tournament size, number of children, estimated generations, mutation probabilities, criteria (X)
3: Load nodes and obstacles from input files
4: Create initial genomes using random Steiner points, Delaunay triangulation, and random corner points
5: Calculate initial total network length
6: Start GA:
7: Make initial genomes
8: Generate population through mutations and crossovers of initial genomes
9: Run GA:
  10: while percentage improvement over last X generations >0.01 do
  11: Generate new population using crossover and mutation
  12: Evaluate fitness of each genome in the population
  13: Update the best solution if a better genome is found
  14: Select genomes for the next generation via tournament selection
  15: end while
16: Output Results:
17: Retrieve the best genome

18: Fine tune the Steiner point locations
19: Calculate and output final network distance

The reader is referred to Rosenberg et al. [14] for further information.

2.2. Formulation of the material balance model

The material balance model is formulated as an optimisation problem with the objective of minimising the network's weighted length L_n^w, as shown in in Equation (3). Let A denote the set of proposed arcs in the network where each arc is represented by an ordered pair of nodes *(i,j)*. The binary variable a_{ij} indicates whether the arc *(i,j)* exists, taking a value of 1 if the arc is included in the network and 0 otherwise. L_{ij}^w represents the length of the arc *(i,j)*.

$$min\ L_n^w = \sum_{(i,j)\in A} a_{ij} \times L_{ij}^w \quad (3)$$

Equation (4) describes the conservation of hydrogen at each node i in the set N, where N denotes the set of nodes in the network. For each node $i \in N$, define the set $K_i = \{k: (k,i) \in A\}$, which represents all nodes k that have arcs directed towards node i. Similarly, define a set J_i such that $J_i = \{j: (i,j) \in A\}$, representing all nodes j that have arcs originating from node i. The variable P_i represents the hydrogen production at node i, and C_i denotes the hydrogen consumption at node i. The term Q_{ki} refers to the incoming hydrogen flowrate from node k to node i, where $k \in K_i$. Similarly, Q_{ij} refers to the outgoing hydrogen flowrate from node i to node j, where $j \in J_i$.

$$\forall i \in N. \quad P_i + \sum_{k\in K_i} Q_{ki} - \sum_{j\in J_i} Q_{ij} - C_i = 0 \quad (4)$$

Equation (5) links the binary decision variable a_{ij} with the flowrate Q_{ij}, ensuring that flow is only possible if the corresponding arc exists. Equation (6) imposes a lower bound on Q_{ij}, maintaining it above a minimal physical threshold when the arc is active. Equation (7) enforces the directionality of connections between nodes, allowing each arc (i,j) to be oriented in only one direction. This constraint also allows for the possibility of eliminating redundant pipelines, enabling the optimisation of the network's structure.

$$\forall (i,j) \in A.\ Q_{ij} - Ma_{ij} \le 0 \quad (5)$$

$$\forall (i,j) \in A.\ Q_{ij} - 0.01a_{ij} \ge 0 \quad (6)$$

$$\forall (i,j) \in A.\ a_{ij} + a_{ji} \le 1 \quad (7)$$

2.3. Formulation of the pipeline sizing optimisation model

The PSO model is built upon the work of Ejeh et al. [31]. Once the network structure and flows are fixed, the pipeline design is optimised with the cost minimisation function given in Equation (8). The network's pipeline capital costs C_{ij}^C are calculated as proposed by Khan et al. [36], expressed in Equation (9). Khan et al. [36] provides several equations for the capital cost's components which are used to generate Fig. 3 that displays the cost component breakdown over a range of outer diameters. The capital costs of each arc $(i,j) \in A$ are a function of the pipeline's outer diameter D_{ij}^{po}, L_{ij}^{w}, and the number of parallel pipes N_{ij}^p. The operating costs are assumed to equate to 4% of the capital costs [19].

$$min\ C = (1+0.04) \sum_{i|(i,j)\in A} C_{ij}^C \quad (8)$$

where

$$\forall (i,j) \in A. \quad C_{ij}^C = N_{ij}^p \left(61e^{2.74D_{ij}^{po}} + 376\left(D_{ij}^{po}\right)^2 + 2290D_{ij}^{po} + 278\right) L_{ij}^w \quad (9)$$

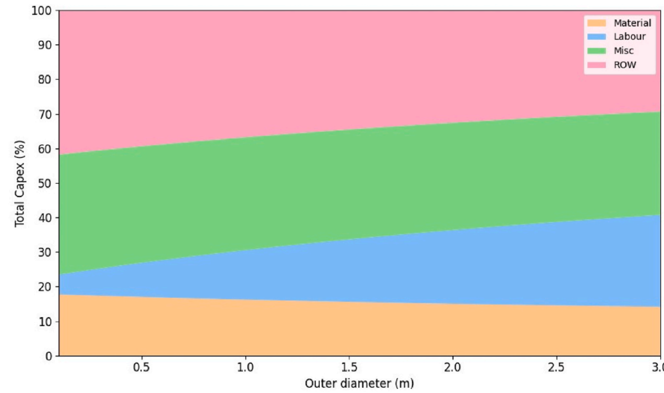

Fig. 3. Percentage distribution of total capital expenditure for pipeline construction based on the outer diameter.

Equation (10) describes the parallel pipeline behaviour along the arc (i,j). The flowrate through each individual pipe Q_{ij}^P on the arc (i,j) is found by dividing the total flowrate Q_{ij}^P by N_{ij}^P, therefore, the flowrate is equal through each parallel pipe on the same arc.

$$\forall (i,j) \in A. \quad Q_{ij}^p = Q_{ij} \Big/ N_{ij}^p \quad (10)$$

The hydraulic behaviour of hydrogen in the pipelines is described by Equations (11)–(14). Equation (11) is a Darcy Weisbach-based equation [37] that defines the pipeline's inner diameter D_{ij}^{pi} on the arc (i,j). The requisites of D_{ij}^{pi} are the pressure differential ΔP_{ij}, friction factor f_{ij}, and Reynold's number Re_{ij}. Equation (12) finds ΔP_{ij} by subtracting the fluid's inflow pressure P_j^{in} at node j from the fluid's outflow pressure P_i^{out} flowing from node i. Equation (13) describes Re_{ij} as a function of Q_{ij}^P, the fluid's dynamic viscosity μ, and D_{ij}^{pi}. Equation (14) is Swamee Jain's approximation of the Colebrook-White equation [38] used to calculate f_{ij}, given as a function of the pipe's roughness ξ, D_{ij}^{pi}, and Re_{ij}.

$$\forall (i,j) \in A. \quad D_{ij}^{pi} = \left(\frac{8f_{ij}{Q_{ij}^p}^2}{\pi^2 \rho \left(\frac{\Delta P_{ij}}{L_{ij}}\right)} \right)^{\frac{1}{5}} \quad (11)$$

$$\forall (i,j) \in A. \quad \Delta P_{ij} = P_i^{out} - P_j^{in} \quad (12)$$

$$\forall (i,j) \in A. \quad Re_{ij} = \frac{4Q_{ij}^p}{\mu \pi D_{ij}^{pi}} \quad (13)$$

$$\forall (i,j) \in A. \quad f_{ij} = \frac{1}{\left(\log_{10}\left(\frac{\xi / D_{ij}^{pi}}{3.7} + \frac{5.74}{Re_{ij}}\right)\right)^2} \quad (14)$$

The pipe's structural constraints are defined by Equations (15)–(20). Equation (15) describes the minimum wall thickness ${t_{ij}}^{wc}$ as a function of D_{ij}^{po}, the minimum yield stress τ^P, design factor κ^{DF}, longitudinal joint factor κ^E, and the pipeline's Maximum Operating Pressure (MOP) P^{MOP}. Equation (16) imposes that the pipeline's wall thickness ${t_{ij}}^w$ must be equal or more than ${t_{ij}}^{wc}$. This is necessary because the available diameters and schedules may inhibit the pipeline from being designed according to its minimum requirements. Equation (17) defines the relationship between D_{ij}^{po}, D_{ij}^{pi}, and t_{ij}^w.

Equations (18)–(20) describe the constraints on the pipeline's commercial availability. Let d denote a set of commercially available diameters. The pipeline's diameters, D_{ij}^{po} and D_{ij}^{pi}, are given as the sum of all products of the commercially viable diameters, D_d^{so} and D_d^{si}, and their corresponding binary activation variable B_d^d. Equation (20) enforces that only one pair of diameters are chosen by fixing B_d^d to equal 1.

$$\forall(i,j)\in A. \quad t^{wc}_{ij} = \frac{P^{MOP} \cdot D^{po}_{ij}}{2\tau^{P}\kappa^{E}\kappa^{DF}} \tag{15}$$

$$\forall(i,j)\in A. \quad t^{w}_{ij} \geq t^{wc}_{ij} \tag{16}$$

$$\forall(i,j)\in A. \quad D^{po}_{ij} = D^{pi}_{ij} + 2 \cdot t^{w}_{ij} \tag{17}$$

$$\forall(i,j)\in A. \quad D^{po}_{ij} = \sum_{d} D^{so}_{d} B^{d}_{ijd} \tag{18}$$

$$\forall(i,j)\in A. \quad D^{pi}_{ij} = \sum_{d} D^{si}_{d} B^{d}_{ijd} \tag{19}$$

$$\forall(i,j)\in A. \quad \sum_{d} B^{d}_{ijd} = 1 \tag{20}$$

Finally, Equation (22) describes the fluid's velocity v^f through the pipeline(s) on arc (i,j) as a function of the fluid's density ρ, Q^p_{ij}, and D^{pi}_{ij}. Equation (23) bounds v^f to be less than or equal to the pipeline's erosion velocity v^e, calculated in Equation (21), to avoid pipe deterioration, where τ^w is the pipeline sheer.

$$\forall(i,j)\in A. \quad v^{e}_{ij} = \sqrt{\frac{8\tau^{w}}{\rho f_{ij}}} \tag{21}$$

$$\forall(i,j)\in A. \quad v^{f}_{ij} = \frac{4Q^{p}_{ij}}{\pi\rho {D^{pi}_{ij}}^{2}} \tag{22}$$

$$\forall(i,j)\in A. \quad v^{f}_{ij} \leq v^{e}_{ij} \tag{23}$$

3. Results and discussion

3.1. Case study

The case study explores hydrogen infrastructure design in the Humber region of the United Kingdom (UK), a key industrial cluster with significant potential for hydrogen energy [39]. Fig. 4 maps the Humber cluster, showing the locations of the producers and consumers.

The industrial site data is sourced from several resources. Both hydrogen producers and consumers are sourced from the UK hydrogen project directory [40] which details active hydrogen projects in the UK. Further data on the hydrogen producers is filtered from the Renewable Energy Planning Database (REPD) [41], which provides information on planned and existing renewable energy projects. Data on the hydrogen consumers was sourced and processed from the NAEI point source emissions database [42]. The hydrogen demands of the consumers are calculated based on typical fuel source compositions in the relevant sector [43] and site-specific publicly available information. Appendix A details the case study's industrial sites with their location, production/uptake and sector.

This case study considers four producers and 23 consumers. Highlighted areas in the region represent the Densely Populated Areas (DPAs), identified as significant geographical obstacles. Additionally, the River Humber is considered a geographical obstacle. DPAs and the River Humber are given a weighting of 2.5 and 10, respectively, based on cost weightings from the literature [16].

Previous industrial projects supporting this cluster have planned and designed an initial hydrogen infrastructure [44] which is used for comparison and discussion, also depicted in Fig. 4 as a blue line with its Above Ground Installations (AGIs). The scope of the infrastructure is limited to pipelines between industrial sites in the Humber cluster; additional pipelines are planned between Easington, Aldbrough, and the Teeside cluster which are considered out-of-scope. Compressor stations are assumed to exist at all sites with hydrogen outflows and at junctions where more than two pipelines converge, with all stations pumping the fluid pressure up to 70 bar. The pipeline design, informed by the National Grid EIA scoping report [45], specifies a maximum diameter of 900 mm and a Maximum Operating Pressure (MOP) between 50 and 75 barg. We consider 817 unique pipeline inner and outer diameter pairs, ranging from DN6 to DN2300 with a wide range of schedules.

3.2. Network design results

Fig. 5 illustrates the full network design using the StObGA method for the network routing and the MINLP sizing model, incorporating geographical, hydraulic, structural and commercial constraints. The route bifurcates into two pipeline trunks to avoid crossing the river at any wide points and navigates around the edges of the densely populated areas. The lower trunk distributes larger hydrogen flows to meet several more sites with high demands, while the upper trunk is longer and serves few industrial sites.

Hydrogen utilisation is categorised into direct and indirect heating processes. However, for the purposes of this analysis, hydrogen used in Direct Reduced Iron (DRI) production within the iron and steel industry is classified under indirect processes. In indirect processes, hydrogen is combusted in gas boilers, and the energy is transferred via another medium, such as water. In direct processes, hydrogen in combusted to produce energy directly for the process, such as in a furnace. Fig. 6 presents two networks where hydrogen supplies only indirect or direct processes to explore the effect on the infrastructure's design. The

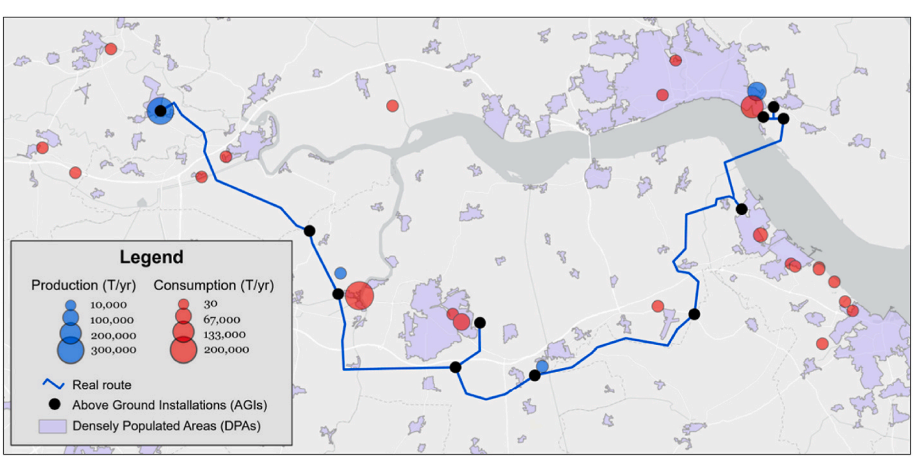

Fig. 4. Potential hydrogen producers (blue) and consumers (red) in the Humber region, UK. Densely populated areas are highlighted as significant geographical constraints. The real route, as defined by National Grid, is depicted [35]. (For interpretation of the references to colour in this figure legend, the reader is referred to the Web version of this article.)

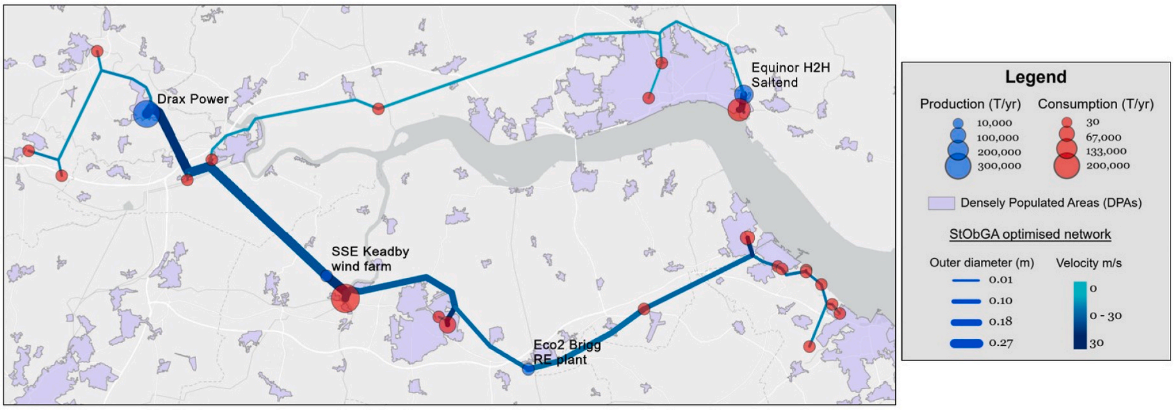

Fig. 5. Snapshot hydrogen infrastructure design for the Humber cluster assuming full hydrogen uptake.

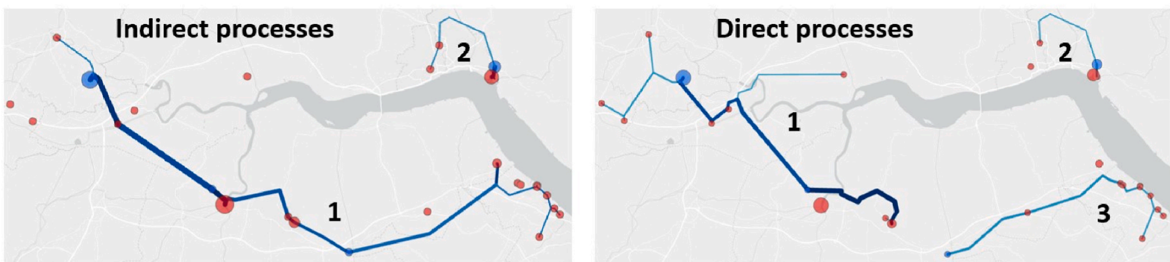

Fig. 6. Comparison of Hydrogen Infrastructure Design for Indirect and Direct Applications. Left: Design optimised for indirect hydrogen applications. Right: Design optimised for direct hydrogen applications.

resulting networks separate into several smaller networks to minimise overall length. In the full network, balancing production and consumption requires a single network to distribute hydrogen satisfactorily. However, reduced demand in alternative scenarios enables the network to segregate.

Table 1 provides a quantitative comparison between the three scenarios and highlights the differences in demand between direct and indirect use-cases in the Humber region. The segregation into several networks results in a lower Levelised Cost of Hydrogen Transportation (LCOHT) for indirect processes.

The large gap in the LCOHT between the direct and indirect networks, compared to the small difference between the full network and indirect processes network, indicates that consumption for indirect processes in large industrial sites is crucial to keeping infrastructure costs low. However, the energy efficiency of hydrogen pathways significantly impacts system-wide performance. Hydrogen used for indirect applications such as boilers suffer higher conversion losses compared to directly electrified alternatives, raising questions about its optimal role within the energy system and highlighting competitive risks that may mitigate hydrogen uptake.

The Technological Readiness Levels (TRLs) for hydrogen in indirect heating applications and the DRI process are more advanced and expected to enter industry imminently, whereas direct applications remain at least a decade away from being ready according to several analyses [46,47]. It is likely that hydrogen-consuming industrial sites will want to utilise hydrogen for both direct and indirect processes. This has implications for the infrastructure's growth as it evolves to meet increasing demand from new applications. Infrastructure designers must contend with the present economic situation of the current design and make allowances for an infrastructure's growth. In this case, the infrastructure should be designed to meet the demand from indirect processes but plan for a future where the full network design will emerge. This aspect requires further investigation, particularly in the infrastructure's routing.

In the analysed scenarios, the economic viability and environmental impact of hydrogen deployment depend significantly on the source of hydrogen and its use cases within the energy system (see Table 2 and Appendix A for detailed information on production technologies). The geographical distribution of production methods further influences the environmental, economic, and technological outcomes of infrastructure design. In this case study, the four producers employ different methods, including biomass gasification, green hydrogen production, and Steam Methane Reforming (SMR) with Carbon Capture, Utilisation, and Storage (CCUS). Biomass gasification and green hydrogen production support the decarbonisation of hard-to-abate sectors and significantly reduce lifecycle greenhouse gas emissions, while SMR with CCUS lowers system-average production costs by leveraging existing fossil fuel

Table 1
Comparison of pipeline network properties and costing results for the full, direct, and indirect scenario networks.

Scenario	Network	Capex ($millions)	Opex ($millions/yr)	Distribution (tonneH2/30yrs)	LCOHT ($/tonneH2)	Total simulation capex ($millions)	Simulation LCOHT ($/tonneH2)
Full network	1	110.261	4.410	12,300,000	20	110.261	20
Indirect processes	1	69.944	2.798	7,600,000	20	81.726	16
	2	11.782	0.471	3,700,000	7		
Direct processes	1	41.485	1.659	900,000	102	65.860	134
	2	16.704	0.668	100,000	365		
	3	7.671	0.307	90,000	196		

Table 2
Estimated production costs and GHG emissions for the designed networks for the full, direct and indirect scenarios.

Scenario	Network	Production costs ($/kgH$_2$)	GHG emissions (kgCO$_2$/kgH$_2$)	Production TRLs
Full network	1	3.44	2.26	5, 7, 8
Indirect processes	1	3.98	0.61	5, 8
	2	2.20	6.00	7
Direct processes	1	3.82	0.67	5, 8
	2	2.20	6.00	7
	3	4.00	0.60	5

resources [48].

These trade-offs between environmental impact, cost, and geographic location pose critical challenges for planners. Unlike natural gas networks, where fuel sources are largely fixed and predictable [49], hydrogen network planning must account for varying locations and production methods, adding layers of complexity. The geographical location and scale of hydrogen production influence not only system-wide economic and environmental outcomes but also the priorities of stakeholders within the energy network. For instance, industrial sites prioritising cost minimisation may resist infrastructure plans favouring green hydrogen producers, while stakeholders with a focus on decarbonisation may advocate for higher-cost, lower-emission alternatives. Addressing these conflicting priorities requires careful coordination to balance competing objectives and align network development with long-term sustainability goals.

From a systemic perspective, the technological constraints of hydrogen infrastructure highlight the readiness of hydrogen systems to support diverse energy applications. In single-producer scenarios, centralised production simplifies integration with existing renewable energy infrastructure, providing efficiencies of scale but potentially limiting adaptability and resilience as demand grows. Conversely, multi-producer systems enhance scalability and redundancy by diversifying supply sources, but they also introduce operational complexities in balancing production, storage, and distribution across dispersed facilities. Furthermore, the intermittent nature of green hydrogen production necessitates larger storage capacities to ensure supply continuity, which increases total system costs and limits the network's scalability [50]. These challenges underscore the need for dynamic and adaptable infrastructure planning that accounts for technological constraints, production variability, and diverse stakeholder priorities.

3.3. Comparative analysis of routing methods

An analysis is performed to compare StObGA against alternative methods, such as a MST using Prim's algorithm and a Steiner tree method. This comparison highlights the importance of considering geographical constraints. Fig. 5 depicts the optimal hydrogen infrastructure design for the Humber cluster, assuming full uptake of hydrogen in the region. This network configuration prefers to avoid the river and minimise entry into urban areas. In contrast, the MST algorithm and Steiner tree, shown in Fig. 7, connect the network without considering geographical constraints, leading to the traversal of the river and DPAs.

Table 3 quantifies the network's length, cost, geographical penalty multiplier, and the adjusted cost when considering the geographical penalties. StObGA increases the length by 27% but reduces the cost by approximately 25% compared to the next best method, the Steiner tree, equating to savings of over $35 million. These differences underscore the structural significance of considering geographical constraints. Qualitatively, site connections and pipeline bends depend on these constraints. These qualitative differences translate into significant quantitative gaps in the network's length and cost. This cost reduction is signficant compared to recent literature aiming to reduce costs through routing improvements. André et al. [9] presents savings of 10–20% over a MST method by iteratively adjusting the route to reduce costs, whereas this study presents savings of over 30% over an MST method.

3.4. Comparative analysis of sizing methods

Fig. 8 presents a cost comparison between different sizing methods for the same route. The first two columns illustrate the costs associated with dynamic velocity optimisation: one using commercially available discrete sizes and the other employing a continuous spectrum of diameters. The implementation of discrete diameters is debated in the literature, but the quantitative impact of these constraints has not been thoroughly investigated. In this case study, the discretisation of pipeline sizes increases the cost by an additional $5 million or 4.3%.

The last four columns in Fig. 8 present fixed velocity scenarios ranging from 5 to 20 m/s in increments of 5 m/s. Expenditure declines as velocity increases, dropping sharply from 5 m/s and then declining more gradually. At 5 m/s, the capital costs are 30% higher than the baseline—dynamic velocity with discrete sizes. The 10 m/s scenario falls within 10% of the baseline, while the 15 m/s scenario costs less than the baseline but more than the dynamic velocity with continuous sizes scenario. The 20 m/s scenario has the lowest costs among the optimisations performed. As the velocity increases in the pipelines, the

Table 3
Cost and length comparison of StObGA, MST and Steiner tree routing methods.

Routing Method	Length (km)	Cost ($million)	Geographical Penalty	Adjusted Cost ($million)
StObGA	161.703	93.544	1.179	110.261
MST	133.012	81.572	1.927	157.197
Steiner tree	129.542	80.079	1.824	146.103

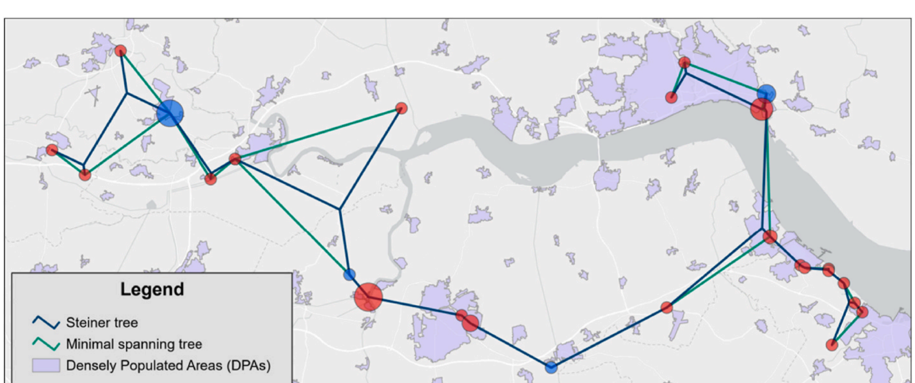

Fig. 7. Minimal spanning tree and Steiner tree topologies.

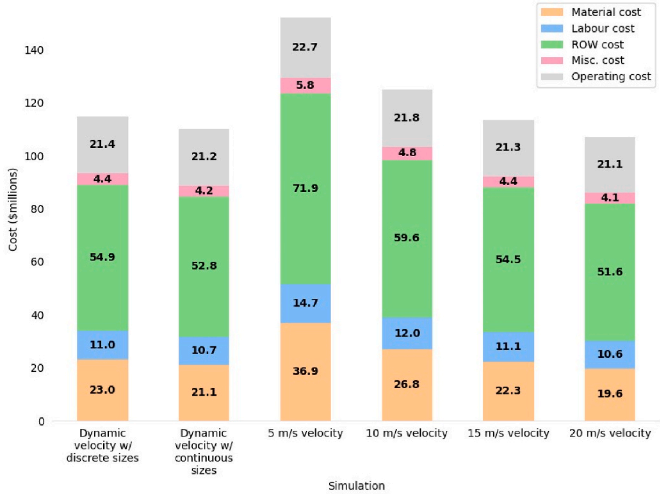

Fig. 8. Stacked bar chart presenting the breakdown of the pipeline's infrastructures capital costs for each sizing scenario with a corresponding cost breakdown.

required pressure drop for a given diameter increases, as does the risk of exceeding the erosional velocity. None of the scenarios exceed the erosional velocity, which ranges between 30 and 60 m/s. However, as velocity increases, the additional compressor power required also rises. Fig. 9 shows the excess pressure drop required in the fixed velocity networks beyond the 40 bar considered in this case study. The most affected pipelines are those with high lengths and small diameters. Pipelines with low flows and high lengths experience particularly extreme excess pressure drops at 20 m/s, exceeding 50 bar. The dynamic velocity scenarios manage the pressure drop by increasing the diameter and reducing the velocity through the pipe.

Fig. 10 shows a selection of outer and inner diameters, along with the corresponding thickness, for a selection of pipelines, providing a detailed depiction and comparison of pipeline diameters (see Appendix B for a full breakdown of the pipeline specifications). This figure demonstrates that as the diameter increases, the variation between the methods also increases. Consequently, for regional and national scales, it becomes more crucial to consider complex constraints. At smaller diameters, which are more commonly observed at local scales, the variation is much smaller and thus has a lesser impact on cost. The trends indicate that fixed velocity networks consistently overestimate the diameter at higher diameter requirements and underestimate the diameters at smaller scales, although the difference is less significant. For this scenario, the best fixed velocity to estimate the cost is 15 m/s. The overcompensation of the wall thickness in the discrete diameter network is particularly noticeable when compared to continuous diameter pipes, with the difference increasing at higher diameters.

3.5. Comparison with the real route

The route designed by the National Grid is compared to the route generated by StObGA in Fig. 11. A visual analysis highlights StObGA's capability in handling geographical constraints and minimising the network's traversal of urban areas, similar to the real route. StObGA learns to compromise its length for cost reductions, increasing the length by 8% compared to a Steiner tree method with a uniform cost surface, resulting in a 40% cost reduction.

The direction taken by StObGA around obstacles matches closely with the real route. However, the real route further increases the network length, suggesting that the cost surface requires additional considerations not accounted for in this study. The differences between the real and StObGA-generated routes are nuanced. Some differences are likely due to geographical constraints not considered in this study, such as roads and train tracks, though the exact motivations remain unknown. Incorporating additional geographical factors such as soil type, wildlife ecology, locations of cultural or geological importance, and traffic complicate routing paths [45]. These limitations could potentially be addressed by including more geographical constraints, either by including more obstacles or using more complex compositions of obstacles. Despite these limitations, it is clear that StObGA is suitable for generating feasible routes in complex geographical terrains.

4. Conclusions

The vast majority of the hydrogen infrastructure projects tracked by the IEA remain in the concept or feasibility study stages. At these stages, the configuration of the infrastructures is subject to deep uncertainty as stakeholders remain non-committal. The ability of decision-makers to generate designs and perform techno-economic analyses for new sites and routes is crucial. However, few studies explore the generation of bespoke, optimal routes that account for complex geographical constraints.

This study addresses this gap by utilising StObGA to find optimal

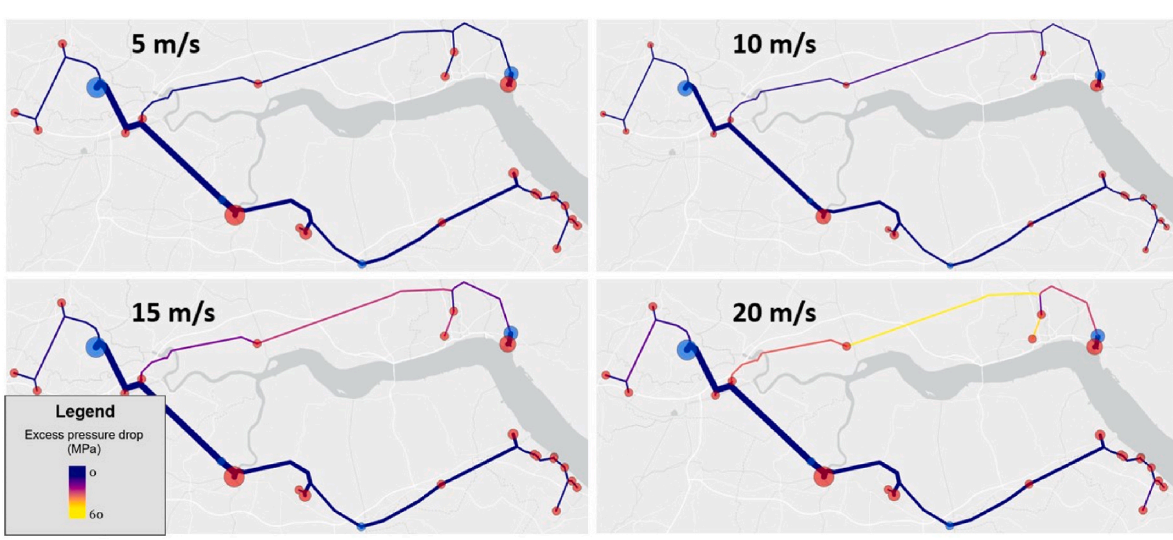

Fig. 9. Hydrogen pipeline infrastructure maps with colour gradient representing the excess pressure drop required to meet the hydraulic requirements. (For interpretation of the references to colour in this figure legend, the reader is referred to the Web version of this article.)

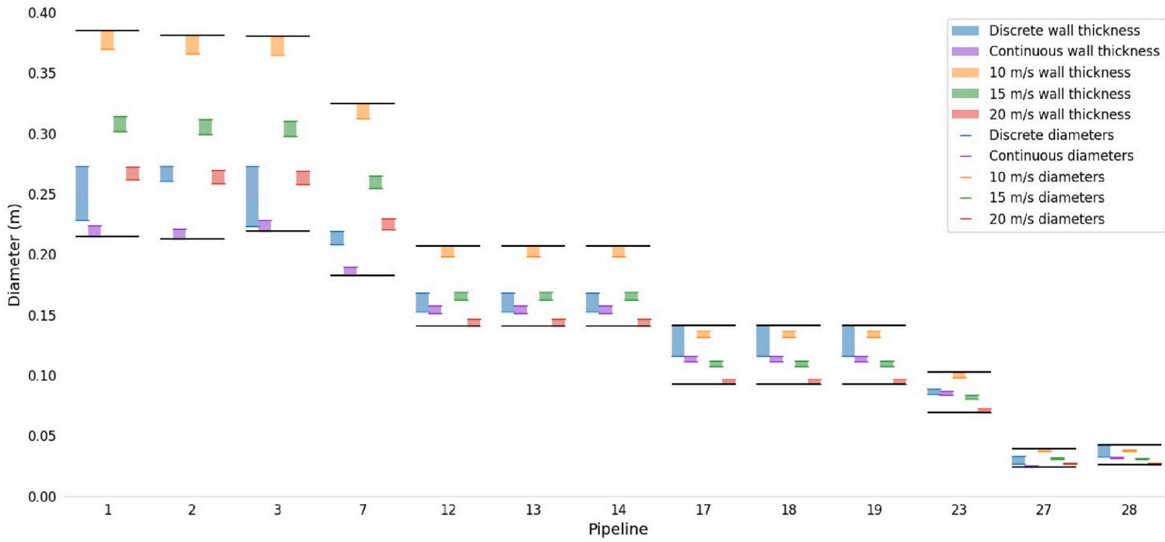

Fig. 10. Diameters and wall thickness from a selection of pipelines from the tested networks.

Fig. 11. A visual comparison of the StObGA-generated route against the real route.

routes for given scenarios. Following this, a high-fidelity MINLP model is employed for pipeline sizing and costing. Using this multi-stage model, we investigate the effect of improving the routing algorithm and sizing optimisation on the infrastructure's cost and design.

The key finding is that the consideration of geographical constraints significantly reduces the infrastructure's capital expenditure by between 20 and 40% compared against previous techniques and aligns with the real route designed by experts. StObGA successfully generates networks with an increased length in order to reduce its cost on an variably-distributed cost surface.

A comparative analysis of various pipeline sizing optimisation configurations is performed to investigate the impact of constraints on the cost and design. Specifically, this study compares discrete and continuous sizing, as well as various fixed velocities. Constraining the optimisation model to commercially available sizes increases the cost by.

4.3%, with the cost difference growing for larger diameters. These results suggest that the cost difference between discrete and continuous sizing is significant for hydrogen infrastructure design between industrial sites. Some argue that future available sizes are unknown; however, it is reasonable to assume that size discretisation will persist and that current commercially available diameters will be a suitable estimate for future sizes.

Previous studies advocate for using a fixed velocity, often 10 or 15 m/s, to estimate pipeline diameters. This study compares several fixed velocities against dynamic velocities in the sizing optimisation, highlighting the limitations of using a fixed velocity for hydrogen infrastructure. The investigation suggests that as the fixed velocity decreases, so does the likelihood of overestimating the diameters for large flows and vice versa. Although the fixed velocity may indicate the accurate overall cost, the design is likely to be sub-optimal.

This multi-stage model serves as a methodology for designing hydrogen infrastructure for a given set of producers, consumers, and variable cost surfaces. This approach differs from other hydrogen energy system models, which often attempt to holistically optimise site selection, equipment, and infrastructural decisions.

In the future, expansions of this work could include increasing the capabilities of the snapshot design model by combining hydrogen-CCUS and hydrogen-heat pipeline infrastructure designs to generate more holistic solutions for industrial clusters. On the other hand, future work could instead direct its focus on extending the model to be suitable for multi-period applications, which may allow for investigations into planning strategies under deep uncertainties in the infrastructure's configuration.

In the future, this work could be expanded by enhancing the snapshot design model by integrating hydrogen-CCUS and hydrogen-heat pipeline infrastructure designs to generate more holistic solutions for industrial clusters. Alternatively, future efforts could focus on extending the model for multi-period applications, enabling investigations of planning strategies under deep uncertainties in the infrastructure's configuration.

CRediT authorship contribution statement

Joseph Hammond: Writing – review & editing, Writing – original draft, Visualization, Methodology, Investigation, Data curation, Conceptualization. **Manou Rosenberg:** Writing – review & editing, Methodology, Conceptualization. **Solomon Brown:** Writing – review & editing, Supervision, Conceptualization.

Funding sources

This research did not receive any specific grant from funding agencies in the public, commercial, or not-for-profit sectors.

Declaration of competing interest

The authors declare that they have no known competing financial interests or personal relationships that could have appeared to influence the work reported in this paper.

Appendix A. Case study details, constraints, and parameters

A1. Input data

Table A1 provides the industrial site data input into the model, including the site, operator, sector, location and production/uptake. As stated in Section 3.1, this data is collated from various sources. The data is processed using the method and values found in Ref. [51].

Table A1
Production and Uptake Data for Various Sites

Site	Operator	Sector/Production Method	Production (kg/yr)	Uptake (kg/yr)	Longitude	Latitude
Grimsby	Novartis grimsby ltd	Pharmaceuticals	–	251,928	−0.117788	53.583828
Great heck	Plasmor ltd	Cement	–	308,950	−1.097508	53.686552
Melton ross	Singleton birch ltd	Lime	–	305,348	−0.364054	53.587179
Hull royal infirmary	Hull university teaching hospitals	Public administration	–	31,886	−0.358218	53.744213
Saltend	BP chemicals ltd	Chemicals	–	2,730,408	−0.238453	53.733631
Goole	Guardian industries ltd	Glass	–	1,065,185	−0.907921	53.698456
Stallingborough	Tronox pigment ltd stallingborough	Chemicals	–	1,327,001	−0.1602	53.616041
Immingham	Knauf UK I	Minerals	–	108,433	−0.19561	53.618828
Grimsby	Tronox pigment ltd immingham	Chemicals	–	238,237	−0.160258	53.614694
Immingham	Knauf UK II	Minerals	–	414,483	−0.190398	53.616951
Stallingborough	Synthomer ltd	Chemicals	–	79,309	−0.141013	53.605407
Rawcliffe bridge	Croda rawcliffe	Chemicals	–	102,578	−0.938592	53.683451
Hull	Croda hull	Chemicals	–	141,263	−0.341623	53.770161
Great coates	Industrial energy services ltd	Chemicals	–	700,277	−0.156067	53.559253
Selby	Sedamyl ltd	Chemicals	–	416,379	−1.052809	53.77894
Scunthorpe	Liberty merchant bar plc	Steel	–	98,926	−0.622434	53.581354
Broomfleet works	Wienerberger ltd	Minerals	–	135,345	−0.698183	53.736181
Grimsby chemical works	BASF	Chemicals	–	79,309	−0.127458	53.590632
Eggborough	Saint-gobain glass ltd	Glass	–	811,268	−1.139104	53.705095
Scunthorpe	British steel ltd	Steel	–	57,800,000	−0.611298	53.575472
Saltend	Saltend cogeneration company ltd	Power	–	123,100,000	−0.244439	53.735517
Immingham	VPI immingham LLP	Power	–	30,000,000	−0.233875	53.640254
Keadby	Keadby generation ltd	Power	–	189,200,000	−0.739847	53.595053
Drax	Drax power	Biomass gasification	260,420,573	–	−0.990414	53.732437
H2H saltend	Equinor H2H saltend	SMR + CCUS	125,267,975	–	−0.238459	53.746877
Brigg RE plant	Eco2 brigg RE plant	Biomass gasification	14,716,800	–	−0.509609	53.542328
Keadby wind farm	SSE keadby wind farm	Wind-driven electrolysis	10,722,240	–	−0.763685	53.611796

A2. Parameters

Table A2 contains parameter values used for the stated case study with references/descriptions of their values.

Table A2
Case study parameter values and corresponding references

Parameter	Value	Unit	Reference
Density	7.85	kg/m^3	Aspen Plus [52] with PENG-ROB method assuming 20C and 25 bar
Dynamic viscosity	0.00000892	Pa s	[53]
Pipe roughness	0.0000178	mm	[54]
Minimum yield stress	4830	bar	[55]
Design factor	0.388	–	[56]
Longitudinal joint factor	1	–	[37]
Maximum operating pressure	75	bar	[45]
Pipeline shear	40	N/m^2	[57]

A3. Production method information

Table A3 contains the production costs, emissions information and technological readiness level values used in the case study with corresponding references.

Table A3
Production Methods, Costs, GHG Emissions, TRL, and References

Production Method	Production Costs ($/kgH$_2$)	GHG Emissions (kgCO$_2$/kgH$_2$)	TRL	References
Biomass gasification	4	0.6	5	[50,58]
Wind-driven electrolysis	3.5	0.8	8	[50,59]
SMR with CCUS	2.2	6	7	[48]

Appendix B. Pipeline design results

Table B1 contains pipeline design results for the full network scenario, which is the primary example design that is referred to throughout the paper. The visualisation of these results can be found in Fig. 5.

Table B1
Pipeline design results for the full network scenario as shown in Fig. 5

ID	From (Lon, Lat)	To (Lon, Lat)	ID (m)	OD (m)	Flow (kg/hr)	Vel (m/s)	Cap Costs ($M)	Op Costs ($M)
0	−0.36405, 53.58718	−0.22763, 53.62719	0.109	0.114	3790	14.3	6.284	7.541
1	−0.98447, 53.73717	−0.97503, 53.73346	0.223	0.273	29553	26.8	0.788	0.945
2	−0.97503, 53.73346	−0.93675, 53.68874	0.223	0.273	29553	26.8	5.881	7.057
3	−0.23846, 53.74688	−0.24123, 53.73639	0.158	0.168	14364	25.8	0.905	1.086
4	−0.76369, 53.61180	−0.73821, 53.59926	0.229	0.273	30544	26.2	2.306	2.767
5	−0.93675, 53.68874	−0.91067, 53.69361	0.260	0.273	29541	19.6	1.903	2.283
6	−0.12746, 53.59063	−0.11779, 53.58383	0.013	0.017	29	7.2	0.375	0.451
7	−0.13419, 53.59115	−0.12746, 53.59063	0.010	0.014	38	15.8	0.167	0.200
8	−1.10168, 53.69825	−1.09751, 53.68655	0.014	0.017	35	8.3	0.504	0.605
9	−1.04752, 53.76474	−1.10168, 53.69825	0.030	0.033	128	6.4	3.443	4.132
10	−0.50961, 53.54233	−0.47008, 53.54862	0.116	0.141	3825	12.8	1.884	2.260
11	−0.47008, 53.54862	−0.40567, 53.56915	0.116	0.141	3825	12.8	3.363	4.035
12	−0.40567, 53.56915	−0.36405, 53.58718	0.116	0.141	3825	12.8	2.368	2.842
13	−0.34162, 53.77016	−0.35822, 53.74421	0.008	0.010	4	2.7	1.118	1.341
14	−0.19561, 53.61883	−0.19040, 53.61695	0.030	0.033	353	17.5	0.169	0.203
15	−0.34435, 53.79199	−0.34162, 53.77016	0.013	0.017	20	5.0	0.922	1.107
16	−0.24123, 53.73639	−0.23845, 53.73363	0.027	0.033	312	19.8	0.150	0.180
17	−0.91067, 53.69361	−0.90792, 53.69846	0.017	0.021	122	18.8	0.222	0.266
18	−0.16061, 53.61517	−0.16020, 53.61604	0.018	0.021	151	21.1	0.039	0.047
19	−0.19040, 53.61695	−0.18510, 53.61257	0.033	0.042	305	13.0	0.265	0.318
20	−0.18510, 53.61257	−0.16061, 53.61517	0.033	0.042	305	13.0	0.726	0.871
21	−0.16026, 53.61469	−0.14101, 53.60541	0.021	0.027	127	13.0	0.660	0.792
22	−0.14101, 53.60541	−0.13419, 53.59115	0.021	0.027	118	12.1	0.664	0.796
23	−0.69818, 53.73618	−0.60345, 53.75597	0.030	0.033	84	4.2	2.776	3.331
24	−0.60345, 53.75597	−0.45557, 53.78674	0.030	0.033	84	4.2	4.330	5.196
25	−0.45557, 53.78674	−0.43840, 53.79133	0.030	0.033	84	4.2	0.520	0.624
26	−0.43840, 53.79133	−0.36007, 53.79334	0.030	0.033	84	4.2	2.165	2.598
27	−0.36007, 53.79334	−0.34435, 53.79199	0.030	0.033	84	4.2	0.438	0.526
28	−0.73821, 53.59926	−0.73314, 53.60156	0.152	0.168	8946	17.0	0.324	0.388
29	−0.73314, 53.60156	−0.72118, 53.60020	0.152	0.168	8946	17.0	0.617	0.741
30	−0.72118, 53.60020	−0.63810, 53.61075	0.152	0.168	8946	17.0	4.307	5.169
31	−0.63810, 53.61075	−0.60608, 53.59937	0.152	0.168	8946	17.0	1.891	2.269
32	−0.60608, 53.59937	−0.60185, 53.58863	0.152	0.168	8946	17.0	0.941	1.129
33	−0.99041, 53.73244	−0.98447, 53.73717	0.260	0.273	29728	19.8	0.692	0.830
34	−0.98447, 53.73717	−0.98563, 53.74490	0.030	0.033	175	8.7	0.362	0.434
35	−0.98563, 53.74490	−0.99125, 53.75223	0.030	0.033	175	8.7	0.375	0.450
36	−0.99125, 53.75223	−1.00828, 53.75841	0.030	0.033	175	8.7	0.552	0.662
37	−1.00828, 53.75841	−1.04752, 53.76474	0.030	0.033	175	8.7	1.124	1.348
38	−0.22763, 53.62719	−0.21449, 53.62239	0.035	0.042	365	13.4	0.450	0.540
39	−0.21449, 53.62239	−0.19561, 53.61883	0.035	0.042	365	13.4	0.578	0.693
40	−0.16061, 53.61517	−0.16026, 53.61469	0.018	0.021	154	21.4	0.023	0.027
41	−0.93675, 53.68874	−0.93680, 53.68861	0.008	0.010	12	8.6	0.005	0.006
42	−0.93680, 53.68861	−0.93859, 53.68345	0.008	0.010	12	8.6	0.212	0.255
43	−0.13419, 53.59115	−0.15607, 53.55925	0.021	0.027	80	8.2	1.543	1.851
44	−1.04752, 53.76474	−1.04763, 53.76504	0.017	0.021	48	7.3	0.013	0.016
45	−1.04763, 53.76504	−1.05281, 53.77894	0.017	0.021	48	7.3	0.616	0.740
46	−0.61209, 53.57851	−0.62243, 53.58135	0.008	0.010	11	8.3	0.273	0.328
47	−0.60185, 53.58863	−0.61209, 53.57851	0.105	0.114	6609	27.1	0.820	0.984
48	−0.91067, 53.69361	−0.90758, 53.70586	0.030	0.033	99	4.9	0.578	0.693
49	−0.90758, 53.70586	−0.88982, 53.71633	0.030	0.033	99	4.9	0.693	0.831

(continued on next page)

Table B1 (*continued*)

ID	From (Lon, Lat)	To (Lon, Lat)	ID (m)	OD (m)	Flow (kg/hr)	Vel (m/s)	Cap Costs ($M)	Op Costs ($M)
50	−0.88982, 53.71633	−0.86630, 53.72089	0.030	0.033	99	4.9	0.684	0.821
51	−0.86630, 53.72089	−0.86181, 53.72079	0.030	0.033	99	4.9	0.124	0.149
52	−0.86181, 53.72079	−0.85330, 53.72884	0.030	0.033	99	4.9	0.443	0.532
53	−0.85330, 53.72884	−0.72709, 53.74296	0.030	0.033	99	4.9	3.551	4.261
54	−0.72709, 53.74296	−0.69818, 53.73618	0.030	0.033	99	4.9	0.859	1.031
55	−1.10168, 53.69825	−1.13910, 53.70510	0.021	0.027	93	9.5	1.040	1.249
56	−0.61209, 53.57851	−0.61130, 53.57547	0.104	0.114	6598	27.3	0.214	0.257
57	−0.24123, 53.73639	−0.24444, 53.73552	0.162	0.168	14053	24.3	0.178	0.214
58	−0.22763, 53.62719	−0.23388, 53.64025	0.076	0.089	3425	26.5	0.844	1.013
59	−0.73821, 53.59926	−0.73985, 53.59505	0.208	0.219	21598	22.5	0.434	0.521
60	−0.34435, 53.79199	−0.34052, 53.79489	0.023	0.027	64	5.3	0.165	0.198
61	−0.34052, 53.79489	−0.32333, 53.80092	0.023	0.027	64	5.3	0.530	0.636
62	−0.32333, 53.80092	−0.25876, 53.78337	0.023	0.027	64	5.3	1.884	2.261
63	−0.25876, 53.78337	−0.23846, 53.74688	0.023	0.027	64	5.3	1.721	2.065
64	−0.91067, 53.69361	−0.76369, 53.61180	0.262	0.273	29320	19.3	14.031	16.838
65	−0.60185, 53.58863	−0.55785, 53.55947	0.084	0.089	2337	13.6	2.438	2.925
66	−0.55785, 53.55947	−0.50961, 53.54233	0.084	0.089	2337	13.6	2.080	2.496

Appendix C. Supplementary data

Supplementary data to this article can be found online at https://doi.org/10.1016/j.ijhydene.2024.12.273.

References

[1] IEA. Global hydrogen review 2023. URL, https://www.iea.org/reports/global-hydrogen-review-2023. [Accessed 16 July 2024].
[2] Frieden F, Leker J. Future costs of hydrogen: a quantitative review. Sustain Energy Fuels 2024;8(9):1806–22. https://doi.org/10.1039/d4se00137k.
[3] Melaina M. Initiating hydrogen infrastructures: analysis of technology dynamics during the introduction of hydrogen fuel for passenger vehicles. PhD Thesis. 2005. p. 11–6. URL, https://hdl.handle.net/2027.42/125448.
[4] IEA. Hydrogen production and infrastructure projects database. URL, https://www.iea.org/data-and-statistics/data-product/hydrogen-production-and-infrastructure-projects-database. [Accessed 16 July 2024].
[5] Grid National. National grid explores plans for UK hydrogen 'backbone'. URL, https://www.nationalgrid.com/national-grid-explores-plans-uk-hydrogen-backbone. [Accessed 16 July 2024].
[6] GasGrid Finland. From vision to action: six partners have signed a cooperation agreement to develop nordic-baltic hydrogen corridor. URL, https://tinyurl.com/2yatkv9v. [Accessed 16 July 2024].
[7] SNAM. Interventions on the energy transition | sheet 1: backbone for hydrogen transport. URL, https://tinyurl.com/3b2ukxn9. [Accessed 16 July 2024].
[8] Heijnen PW, Chappin EJ, Herder PM. A method for designing minimum-cost multisource multisink network layouts. Syst Eng 2019;23(1):14–35. https://doi.org/10.1002/sys.21492.
[9] André J, Auray S, Brac J, Wolf DD, Maisonnier G, Ould-Sidi M-M, Simonnet A. Design and dimensioning of hydrogen transmission pipeline networks. Eur J Oper Res 2013;229(1):239–51. https://doi.org/10.1016/j.ejor.2013.02.036.
[10] Baufumé S, Grüger F, Grube T, Krieg D, Linssen J, Weber M, Hake J-F, Stolten D. GIS-based scenario calculations for a nationwide German hydrogen pipeline infrastructure. Int J Hydrogen Energy 2013;38(10):3813–29. https://doi.org/10.1016/j.ijhydene.2012.12.147.
[11] Reuß M, Welder L, Thürauf J, Linßen J, Grube T, Schewe L, Schmidt M, Stolten D, Robinius M. Modeling hydrogen networks for future energy systems: a comparison of linear and nonlinear approaches. Int J Hydrogen Energy 2019;44(60):32136–50. https://doi.org/10.1016/j.ijhydene.2019.10.080.
[12] Joseph B, Kruskal Jr. On the shortest spanning subtree of a graph and the traveling salesman problem. In: Proceedings of the American mathematical society, vol. 7. American Mathematical Society; 1956. p. 48–50. https://doi.org/10.2307/2033241.
[13] Prim RC. Shortest connection networks and some generalizations. Bell Syst Tech J 1957;36. https://doi.org/10.1002/j.1538-7305.1957.tb01515.x.
[14] Rosenberg M, French T, Reynolds M, While L. A genetic algorithm approach for the euclidean steiner tree problem with soft obstacles. In: Proceedings of the genetic and evolutionary computation conference. ACM; 2021. https://doi.org/10.1145/3449639.3459397.
[15] Becattini V, Gabrielli P, Antonini C, Campos J, Acquilino A, Sansavini G, Mazzotti M. Carbon dioxide capture, transport and storage supply chains: optimal economic and environmental performance of infrastructure rollout. Int J Greenh Gas Control 2022. https://doi.org/10.1016/j.ijggc.2022.103635.
[16] van den Broek M, Mesquita P, Carneiro J, Silva JR, Berghout N, Ramírez A, Gouveia JP, Seixas J, Cabal H, Martinez R, Rimi A, Zarhloule Y, Sardinha M, Boavida D, Tosato G. Region specific challenges of a co2 pipeline infrastructure in the west mediterranean sea. Energy Proc 2013;37:3137–46. https://doi.org/10.1016/j.egypro.2013.06.200.
[17] Heijnen PW, Ligtvoet A, Stikkelman RM, Herder PM. Maximising the worth of nascent networks. Network Spatial Econ 2013;14(1):27–46. https://doi.org/10.1007/s11067-013-9199-1.
[18] Johnson N, Ogden J. A spatially-explicit optimization model for long-term hydrogen pipeline planning. Int J Hydrogen Energy 2012;37(6):5421–33. https://doi.org/10.1016/j.ijhydene.2011.08.109.
[19] Parolin F, Colbertaldo P, Campanari S. Development of a multi-modality hydrogen delivery infrastructure: an optimization model for design and operation. Energy Convers Manag 2022;266. https://doi.org/10.1016/j.enconman.2022.115650.
[20] N. Balta-Ozkan, E. Baldwin, Spatial development of hydrogen economy in a low-carbon UK energy system 38 (3) 1209–1224. doi:10.1016/j.ijhydene.2012.11.049.
[21] Cowley T, Hutty T, Hammond J, Brown S. Achieving emissions reduction through the utilisation of local low-grade heat sources in district heat networks. Appl Therm Eng 2024. https://doi.org/10.1016/j.applthermaleng.2024.122381.
[22] Middleton RS, Kuby MJ, Bielicki JM. Generating candidate networks for optimization: the co_2 capture and storage optimization problem. Comput Environ Urban Syst 2012;36(1):18–29. https://doi.org/10.1016/j.compenvurbsys.2011.08.002.
[23] Middleton RS, Yaw SP, Hoover BA, Ellett KM. Simccs: an open-source tool for optimizing co_2 capture, transport, and storage infrastructure. Environ Model Software 2020;124:104560. https://doi.org/10.1016/j.envsoft.2019.104560.
[24] Kuby MJ, Middleton RS, Bielicki JM. Analysis of cost savings from networking pipelines in ccs infrastructure systems 4. 2011. p. 2808–15. https://doi.org/10.1016/j.egypro.2011.02.185.
[25] Yang C. Ogden, Determining the lowest cost hydrogen delivery mode. Int J Hydrogen Energy 2008. https://doi.org/10.1016/j.ijhydene.2006.05.009.
[26] Department for Business. Energy and industrial strategy, hydrogen strategy update to the market: july 2022. URL, https://assets.publishing.service.gov.uk/media/64c7e9125c2e6f0013e8d7ea/hydrogen-strategy-update-to-the-market-july-2022.pdf; 2022.
[27] Welder L, Ryberg D, Kotzur L, Grube T, Robinius M, Stolten D. Spatio-temporal optimization of a future energy system for power-to-hydrogen applications in Germany. Energy 2018;158:1130–49. https://doi.org/10.1016/j.energy.2018.05.059.
[28] Robinius M, Schewe L, Schmidt M, Stolten D, Thürauf J, Welder L. Robust optimal discrete arc sizing for tree-shaped potential networks. Comput Optim Appl 2019;73(3):791–819. https://doi.org/10.1007/s10589-019-00085-x.
[29] Weber A, Papageorgiou L. Design of hydrogen transmission pipeline networks with hydraulics. Chem Eng Res Des 2018;131:266–78. https://doi.org/10.1016/j.cherd.2018.01.022.
[30] Middleton R, Bielicki J. A scalable infrastructure model for carbon capture and storage: simccs. Energy Pol 2009;37:1052–60. https://doi.org/10.1016/j.enpol.2008.09.049.
[31] Ejeh J, Martynov S, Brown S. An minlp model for the optimal design of co2 transportation infrastructure in industrial clusters. Comput Aided Chem Eng 2023;52:3085–90. https://doi.org/10.1016/b978-0-443-15274-0.50492-3.
[32] Dayhim M, Jafari MA, Mazurek M. Planning sustainable hydrogen supply chain infrastructure with uncertain demand. Int J Hydrogen Energy 2014;39(13):6789–801. https://doi.org/10.1016/j.ijhydene.2014.02.132.
[33] Parolin F, Colbertaldo P, Campanari S. Optimal design of hydrogen delivery infrastructure for multi-sector end uses at regional scale. Int J Hydrogen Energy 2024;79:839–49. https://doi.org/10.1016/j.ijhydene.2024.06.049.

[34] Emodi NV, Lovell H, Levitt C, Franklin E. A systematic literature review of societal acceptance and stakeholders' perception of hydrogen technologies. Int J Hydrogen Energy 2021;46(60):30669–97. https://doi.org/10.1016/j.ijhydene.2021.06.212.
[35] Hammond J, Rosenberg M, Brown S. A genetic algorithm-based design for hydrogen pipeline infrastructure with real geographical constraints. Comput Aided Chem Eng 2024;53:631–6. https://doi.org/10.1016/b978-0-443-28824-1.50106-x.
[36] Khan M, Young C, Layzell D. The techno-economics of hydrogen pipelines, Tech. rep. Transition Accelerator Technical Briefs; 2021.
[37] Mechleri E, Brown S, Fennell PS, Dowell NM. CO2 capture and storage (CCS) cost reduction via infrastructure right-sizing. Chem Eng Res Des 2017;119:130–9. https://doi.org/10.1016/j.cherd.2017.01.016.
[38] Swamee PK, Jain AK. Explicit equations for pipe-flow problems. J Hydraul Div 1976. https://doi.org/10.1061/jyceaj.0004542.
[39] Department for Business. Energy and industrial strategy, industrial decarbonisation strategy. URL, https://www.gov.uk/government/publications/industrial-decarbonisation-strategy; 2021.
[40] Gemserv. Hydrogen project directory. URL, https://projectmap.hydrogen-uk.org/; 2024.
[41] Department for Business. Energy and industrial strategy. Renew Energy Plan Database 2022. URL, https://www.gov.uk/government/publications/renewable-energy-planning-database-monthly-extract.
[42] Department for Business. Energy and Industrial Strategy, Naei point source emitters database. URL, https://naei.beis.gov.uk/data/map-large-source; 2021.
[43] Gailani A, Cooper S, Allen S, Pimm A, Taylor P, Gross R. Assessing the potential of decarbonization options for industrial sectors. Joule 2024;8(3):576–603. https://doi.org/10.1016/j.joule.2024.01.007.
[44] Grid National. Humber low carbon pipelines project: section maps of the proposed route for consultation. URL, https://www.nationalgrid.com/our-businesses/national-grid-ventures/humber-low-carbon-pipelines/documents; 2022.
[45] National Grid. Humber low carbon pipelines environmental impact assessment scoping report. URL, https://infrastructure.planninginspectorate.gov.uk/wp-content/ipc/uploads/projects/EN070006/EN070006-000026-HLCP-ScopingReportVolumeI.pdf; 2022.
[46] Draxler M, Sormann A, Kempken T, Hauck T, Pierret J-C, Borlee J, Donato D, De Santis M, Wang C. Technology assessment and roadmapping (deliverable 1.2). URL D1-2_-Assessment_and_roadmapping_of_technologies_-Publishable-version.pdf, https://www.estep.eu/assets/Projects/GreenSteel4Europe/GreenSteel_Publication/210308_D1-2_-Assessment_and_roadmapping_of_technoogies_-Publishable-version.pdf; 2021.
[47] ARUP. Study to develop cost and stock assumptions for options to enable or require hydrogenready industrial boilers. URL, https://assets.publishing.service.gov.uk/media/6396e0c2e90e0769b9c8dad7/External_research_study_hydrogen-ready_industrial_boilers.pdf; 2022.
[48] Mullen D, Herraiz L, Gibbins J, Lucquiaud M. On the cost of zero carbon hydrogen: a techno-economic analysis of steam methane reforming with carbon capture and storage. Int J Greenh Gas Control 2023;126:103904. https://doi.org/10.1016/j.ijggc.2023.103904.
[49] Arapostathis S, Pearson PJ, Foxon TJ. UK natural gas system integration in the making, 1960–2010: complexity, transitional uncertainties and uncertain transitions. Environ Innov Soc Transit 2014;11(technical):87–102. https://doi.org/10.1016/j.eist.2014.01.004.
[50] Kyriakopoulos GL, Aravossis KG. Literature review of hydrogen energy systems and renewable energy sources. Energies 2023;16:7493. https://doi.org/10.3390/en16227493.
[51] Biggins F, Hutty T, Cowley T, Brown S. Hydrogen conversion and grid capacity for south yorkshire. URL, https://www.sheffield.ac.uk/office-for-data-analytics/hydrogen-conversion; 2022.
[52] Aspen Technology Inc. Aspen plus software, process simulation and modelling software. URL, https://www.aspentech.com; 2019.
[53] Muzny C, Huber M, Kazakov A. Correlation for the viscosity of normal hydrogen obtained from symbolic regression, vol. 58; 2013. p. 969–79. https://doi.org/10.1021/je301273j.
[54] McCoy S, Rubin E. An engineering-economic model of pipeline transport of co2 with application to carbon capture and storage. Int J Greenh Gas Control 2008-04; 2(2):219–29. https://doi.org/10.1016/s1750-5836(07)00119-3.
[55] Cerniauskas S, Grube T, Praktiknjo A, Stolten D, Robinius M. Future hydrogen markets for transportation and industry: the impact of co_2 taxes. Energies 2019;12 (24):4707. https://doi.org/10.3390/en12244707.
[56] Wang B, Liang Y, Zheng J, Qiu R, Yuan M, Zhang H. An milp model for the reformation of natural gas pipeline networks with hydrogen injection. Int J Hydrogen Energy 2018;43(33):16141–53. https://doi.org/10.1016/j.ijhydene.2018.06.161.
[57] American Petroleum Institute. Recommended practice for the design and installation of offshore production platform piping systems. fifth ed. 1991.
[58] Rosa L, Mazzotti M. Potential for hydrogen production from sustainable biomass with carbon capture and storage. Renew Sustain Energy Rev 2022;157:112–23. https://doi.org/10.1016/j.rser.2022.112123.
[59] Department for Business, Energy and Industrial Strategy, Hydrogen production costs 2021. URL https://www.gov.uk/government/publications/hydrogen-production-costs-2021.